Spatially Resolved Measurement of Inhomogeneous Electrocoloration/Insertion in Polycrystalline Molybdenum Oxide Thin Films via Chronoabsorptometric Imaging

Todd M. McEvoy and Keith J. Stevenson*

Department of Chemistry and Biochemistry, University of Texas at Austin, Austin, Texas 78712

Received March 28, 2003; E-mail: stevenson@mail.cm.utexas.edu

Here, using the combination of electrochemical potential step perturbation and time-lapse transmission optical microscopy, we report a new approach for resolving localized charge transfer and transport processes in inhomogeneous transition-metal oxides. Importantly, for the first time, we describe the simultaneous measurement of spatially resolved diffusion coefficients and ionic conductivities for localized regions of distinct chemical composition in polycrystalline MoO_3.

Redox-active metal oxides (e.g., WO_3 and MoO_3) are interesting materials for electrochemical devices such as nonemissive displays[1] and secondary lithium batteries.[2] The basic reaction mechanism involves the simultaneous electrochemical injection of electrons and charge compensating cations (H^+ or Li^+) to produce a colored state, e.g., $Mo^{VI}O_3$ (transparent) $+ xe^- + xLi^+ \rightleftharpoons Li_xMo^{VI}_{1-x}Mo^V_xO_3$ (blue), where chromic changes result from intervalence-type optical transitions.[1] As discussed by Rolison and Dunn in a recent review,[3] disordered materials demonstrate faster ionic transport and increased charge storage capacities in comparison to their crystalline or coarse-grained analogues. For instance, studies of MoO_3 aerogels that possess both amorphous and nanocrystalline characteristics display increased lithium capacities (~1.5 Li^+ per host metal atom) and higher energy densities.[4] Disordered materials of this nature are difficult to characterize because they do not possess long-range order, contain morphological inhomogeneities (e.g., networks, tunnels, and dislocations), and have unique compositions and defect chemistry (e.g., mixed-valency, oxygen deficiencies, and cation vacancies).

Knowledge of intercalate diffusion coefficients in electrochromic/insertion materials is vital for understanding coloration and charge transfer behavior since the kinetics of the electrochemical redox change are typically dictated by the rate of ion transport. In this regard, substantial efforts have been made to estimate diffusion coefficients using numerous experimental methods such as cyclic voltammetry, chronoamperometry, electrochemical impedance spectroscopy, and potentiostatic intermittent titration techniques (PITT).[5,6] Others, such as Bohnke[7] and Decker[8] have coupled spectrochemical with electrochemical methods to investigate solid-state diffusion processes occurring in amorphous WO_3. However, a main disadvantage of these techniques is that they provide only an ensemble-averaged estimation of the transport kinetics since the measured response (e.g., charge or absorbance) is proportional to the integrated concentration of homogeneously distributed redox sites. As demonstrated herein, for investigations of disordered heterogeneous materials, better comprehension of controlling factors can be significantly aided by spatially resolved measurements to reduce ambiguity and allow for direct correlation between structure, distribution, composition, and localized reactivity.

Molybdenum oxide thin films used in this study were prepared[9,10] by cathodic electrodeposition onto indium−tin oxide (ITO) electrodes and subsequently sintered at 250 °C in air for 3 h. The
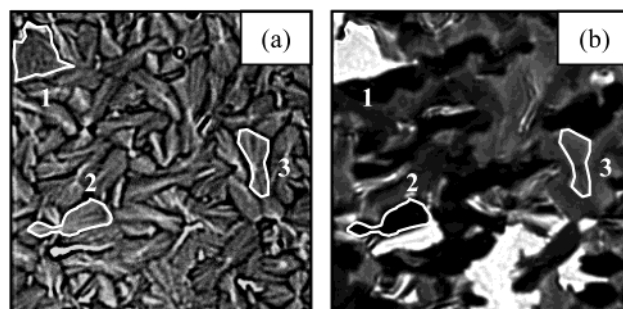

Figure 1. Chronoabsorptometric imaging of Li^+ insertion at a MoO_3/ITO electrode immersed in 1 M $LiClO_4$/PC. Optical micrographs (75×75 μm^2) of (a) at an initial oxidized state ($+0.4$ V vs Ag/AgCl, 0 s) and (b) at a reduced state (-0.8 V, 20 s). Selected regions of interest (ROIs) are highlighted, illustrating varying degrees of coloration/insertion for distinguished phases.

resultant films were transparent with thicknesses of 120 ± 10 nm as determined by AFM. As reported previously,[11] AFM, XRD, and Raman spectroscopy studies indicate that these films consist of randomly dispersed polycrystalline domains of α- and β-MoO_3. A cyclic voltammogram (CV) obtained at a MoO_3/ITO electrode in 1 M $LiClO_4$/PC displays multiple Li^+ insertion/de-insertion peaks during initial cycling which is suggestive of energetically distinct, domain specific reactivity (Supporting Information). As discussed in detail,[11] the shape of the CV changes considerably after the first scan due to an insertion induced irreversible structural transformation and implies that the MoO_3 becomes more disordered but is cycled reversibly in a quasiamorphous state.

To better understand this complex voltammetric behavior, we employed a newly developed spectroelectrochemical methodology to probe localized electrochemical reaction kinetics and monitor morphological changes. Since the charge transfer reaction involves a simultaneous visible change in the optical density of the material, the electrochromic response is used to monitor the lithium insertion behavior. Such an experiment, which we term chronoabsorptometric imaging, is shown in Figure 1, where time-lapsed transmitted light images ($\lambda = 630$ nm) were collected as a function of time following application of a potential step from an oxidizing potential ($+0.4$ V, de-inserted state) to a subsequent reducing potential (-0.8 V, inserted state). For better visualization, a movie of this imaging experiment can be viewed by accessing our Internet website.[12] Briefly, images for pristine MoO_3 films prior to insertion are transparent and consist of randomly oriented grains of dispersed size, orientation, and crystallinity (Figure 1a). Examination of the time-lapsed images reveals that structural changes occur during initial lithium insertion, as is also inferred by the observed changes in the cycle-dependent CV response. Images of reduced films (Figure 1b) exhibit variegated behavior. For illustrative purposes, in Figure 1 we highlight three different regions of interest (ROIs)
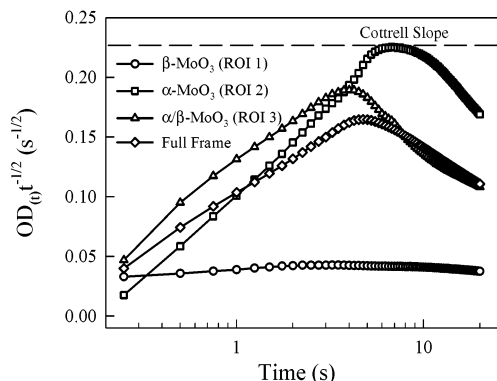
Figure 2. $OD_{(t)}t^{-1/2}$ vs log t plot for denoted regions of interest (ROIs) and the ensemble-averaged (full frame) optical response from Figure 1.

that denote unique areas of inhomogeneous coloration/insertion. Ex situ Raman microprobe spectroscopy experiments (data not shown) performed prior to these optical imaging studies indicate that regions that appear bright (more transmissive) undergo the least amount of coloration (ROI 1) and consist primarily of nanocrystalline monoclinic β-MoO$_3$, while domains that appear dark (more absorptive) undergo the largest coloration (ROI 2) and are composed of predominantly orthorhombic α-MoO$_3$. Regions characterized by an intermediate degree of coloration (ROI 3) consist of disordered mixtures of both α- and β-MoO$_3$. The correlation of the domain specific chemical composition with localized electrochemical behavior enables us to directly estimate the relative contributions of each identified phase by simply thresholding pixel intensities of the images at specific coloration levels. The estimated electroactive areas for coloration/insertion of these distinguished phases were found to be 49.0, 12.2, and 38.8% for α-MoO$_3$, β-MoO$_3$, and mixed-phase α/β-MoO$_3$ domains, respectively.

Quantitative estimates of spatially resolved insertion kinetics can be determined by calculating the average pixel intensity within each distinguished phase (illustrated by labeled ROIs) as a function of time and converting these values to localized optical densities (OD), OD $= \log(I_0/I_q)$, where, I_0 and I_q are the initial and time-dependent average pixel intensities, respectively. Moreover, apparent chemical diffusion coefficients, D_{OD}, can be estimated by using a derived optical expression analogous to the well-known Cottrell equation, ($OD_{(t)}t^{-1/2} = 2D_{OD}^{1/2}\Delta OD\pi^{-1/2}L^{-1}$), where, ΔOD is the overall optical density change and L is the film thickness (Supporting Information). As described by Montella[13] and others,[14] creating a plot of $OD_{(t)}t^{1/2}$ vs log t (Figure 2) allows for visualization of the different diffusional time regimes (ultrashort, short, and long), which correspond to distinct steps in the coloration/insertion process. The ultrashort time region is associated with MoO$_3$/ITO/solution interfacial charging effects. The long time regime ($t > L^2/D$) is associated with redox site saturation and the finite space effect. The short time region, controlled by semi-infinite planar diffusion, presents itself as a plateau in the $OD_{(t)}t^{1/2}$ vs log t plot and corresponds to the Cottrell region. D_{OD} values can be calculated either from the plateau of the $OD_{(t)}t^{1/2}$ vs log t plot (Cottrell slope) or, equivalently, from the slope of a linear plot of $OD_{(t)}$ vs $t^{1/2}$. Regardless, D_{OD} values for each of the corresponding phases and the ensemble-averaged response in Figure 1 were found to be $7.4_7 \times 10^{-12}$, $1.0_2 \times 10^{-11}$, $1.7_6 \times 10^{-11}$, and $1.2_8 \times 10^{-11}$ cm^2/s for β-MoO$_3$ (ROI 1), α-MoO$_3$ (ROI 2), mixed-phase α/β-MoO$_3$ (ROI

3), and ensemble-averaged (full frame) portions, respectively. These results are in agreement with the broad range of values reported for polycrystalline α-/β-phase (10^{-9} to 10^{-11})[15,16] and crystalline α-phase (10^{-9} to 10^{-11})[16,17] MoO$_3$. To our knowledge, we are the first to report a diffusion coefficient for metastable β-MoO$_3$. D_{OD} values also can be used to estimate localized ionic conductivities using the Nernst–Einstein relation ($\sigma = Ne^2D/kT$, where D is the chemical diffusion coefficient and N is the number of ions per unit volume). The ionic conductivities were found to be $1.1_0 \times 10^{-6}$, $1.8_0 \times 10^{-7}$, and $1.2_1 \times 10^{-6}$ S/cm for α-, β-, and mixed-phase α/β-MoO$_3$ domains, respectively. Furthermore, localized Li$^+$ insertion ratios (x in Li$_x$Mo$^{VI}_{1-x}$Mo^V_xO$_3$) can also be determined from the images with values found to be 0.88, 0.22, and 0.59 Li$^+$/MoO$_3$ for α-, β-, and mixed-phase α/β-MoO$_3$, respectively.

A more thorough account of this complex behavior is forthcoming.[18] However, a key aspect to recognize is that the overall coloration/insertion response does not simply constitute the weighted average of all regions. Instead, isolated domains of this polymorphous material exhibit unique reaction kinetics complicated by ohmic potential drop effects and by the influence of compositional gradients imposed by evolving structural changes. As illustrated herein, spatiotemporal measurements have unveiled the richness and complexity of ion/charge-transfer reactivity in polycrystalline MoO$_3$ that previous studies using conventional ensemble-averaging techniques have either missed or inadequately characterized. Future application of this methodology will contribute to the improved understanding of disordered inhomogeneous materials and foster the development of advanced modeling/simulation techniques for extracting and predicting optical, ionic, electronic, and mass transport properties.

Supporting Information Available: Experimental details, figure showing the CV for a MoO$_3$/ITO electrode, and derivation of the time-dependent optical density equation. This material is available free of charge via the Internet at http://pubs.acs.org.

References

(1) Granqvist, C. G. *Handbook of Inorganic Electrochromic Materials*, 1st ed.; Elsevier: New York, 1995.
(2) Schöllhorn, R. *Angew. Chem., Int. Ed. Engl.* **1980**, *19*, 983−1003.
(3) Rolison, D. R.; Dunn, B. *J. Mater. Chem.* **2001**, *11*, 963−980.
(4) Dong, W.; Mansour, A. N.; Dunn, B. *Solid State Ionics* **2001**, *144*, 31−40.
(5) Bard, A. J.; Faulkner, L. *Electrochemical Methods* Wiley: New York, 2001.
(6) Wen, C. J.; Boukamp, B. A.; Huggins, R. A.; Weppner, W. *J. Electrochem. Soc.* **1979**, *126*, 2258−2266.
(7) Vuillemin, B.; Bohnke, O. *Solid State Ionics* **1994**, *68*, 257−267.
(8) Van Driel, F.; Decker, F.; Simone, F.; Pennisi, A. *J. Electroanal. Chem.* **2002**, *537*, 125−134.
(9) Guerfi, A.; Paynter, R. W.; Dao, L. H. *J. Electrochem. Soc.* **1995**, *142*, 3457−3464.
(10) McEvoy, T. M.; Stevenson, K. J. *Anal. Chim. Acta* **2003**, in press.
(11) McEvoy, T. M.; Stevenson, K. J.; Hupp, J. T.; Dang, X. *Langmuir* **2003**, *19*, 4316−4326.
(12) http://neon.cm.utexas.edu/stevenson/JACS2003.
(13) Montella, C. *J. Electroanal. Chem.* **2002**, *518*, 61−83.
(14) Levi, M. D.; Lu, Z.; Aurbach, D. *Solid State Ionics* **2001**, *143*, 309−318.
(15) Guzman, G.; Yebka, B.; Livage, J.; Julien, C. *Solid State Ionics* **1996**, *86−88*, 407−413.
(16) Julien, C.; Nazri, G. A. *Solid State Ionics* **1994**, *68*, 111−116.
(17) Julien, C.; El-Farh, L.; Balkanski, M.; Hussain, O. M.; Nazri, G. A. *Appl. Sur. Sci.* **1993**, *65−66*, 325−330.
(18) McEvoy, T. M.; Stevenson, K. J. Manuscript in preparation.

JA035370C